J Wood Sci (2008) 54:362–368
DOI 10.1007/s10086-008-0962-8

© The Japan Wood Research Society 2008

ORIGINAL ARTICLE

Ali Awaludin · Takuro Hirai · Toshiro Hayashikawa
Yoshihisa Sasaki

Load-carrying capacity of steel-to-timber joints with a pretensioned bolt

Received: September 21, 2007 / Accepted: March 27, 2008 / Published online: May 21, 2008

Abstract Previous experimental studies reported that bolt pretensioning greatly increases the initial stiffness and load-carrying capacity of bolted joints. It is also a matter of great importance to structural designers to understand the effect of pretension on the load-carrying capacities of bolted joints, and this study presents an extended yield model that considers the fastener's pretension force. In the extended yield model, the load-carrying capacity was defined as the load at a slip of 15 mm. The ultimate fastener bending angle at the yielded cross section equivalent to this joint slip, which was affected by the fastener's axial force, was iteratively evaluated in numerical analyses. The introduction of bolt pretensioning largely increased the joint slip resistance at initial loading, but it decreased the ultimate fastener bending angle. This decrease of fastener bending angle resulted in a relatively low stiffness hardening (or secondary stiffness), which is caused by secondary axial forces associated with embedment of steel plates into the wood member. Prediction was verified by the tests of 36 steel-to-timber joints under three different pretension forces and two loading directions relative to the grain. Some of the observed load-carrying capacities of the joints, particularly in loading perpendicular to the grain, however, were not as high as those expected by the numerical analyses considering the given pretension forces.

Key words Load-carrying capacity · Pretensioned bolt · Timber joint · Yield model

A. Awaludin (✉)
Laboratory of Bridge and Structural Design Engineering, Graduate School of Engineering, Hokkaido University, Kita 13 Nishi 8, Kita-Ku, Sapporo 060-8628, Japan
Tel. +81-11-706-6170; Fax +81-11-757-8159
e-mail: awaludin@eng.hokudai.ac.jp

T. Hirai · Y. Sasaki
Graduate School of Agriculture, Hokkaido University, Sapporo 060-8589, Japan

T. Hayashikawa
Graduate School of Engineering, Hokkaido University, Sapporo 060-8628, Japan

Introduction

Timber joints have been intensively investigated owing to their importance in terms of strength, ductility, and energy dissipation of engineered timber constructions. A concept similar to a prestressing technique,[1,2] which was originally applied to improve the structural performance of laminated wood decks of timber bridges, gives an increment in initial stiffness of dowel-type connections by introducing pretension force to their fasteners.[3,4] Moreover, bolt pretensioning also largely enhanced hysteretic damping (area enclosed by a hysteretic loop) and did not give negative effects on joint ductility, which are important factors for buildings to survive earthquakes. In our previous study,[4] however, it was found that this significant increase of initial stiffness was followed by a slight increase of ultimate resistance, of about 10%. Investigation of single-bolt connections is required to clarify this finding.

The main objective of this study was to evaluate the effects of pretension force in bolt on the load-carrying capacity of steel–wood–steel joints. The connection load–slip curve was analyzed with finite element code DOWEL,[5] while the joint load-carrying capacity was evaluated by the yield model with additional analysis to take the fastener's axial force into consideration. The analytical results were verified by conducting single-bolt connection tests under three different pretension forces and using two loading directions relative to the grain. A slender bolt was intentionally used in the experiment because this type of dowel fastener has a higher energy dissipation capacity than a stiff bolt.

Extended yield model

Adopted from the EC5,[6] Fig. 1 shows two possible failure modes for steel-to-timber joints in double shear with one slender dowel-type fastener. Expressions to compute dowel bearing strength of wood (f_e) for loading directions parallel and perpendicular to the grain can be found in some design

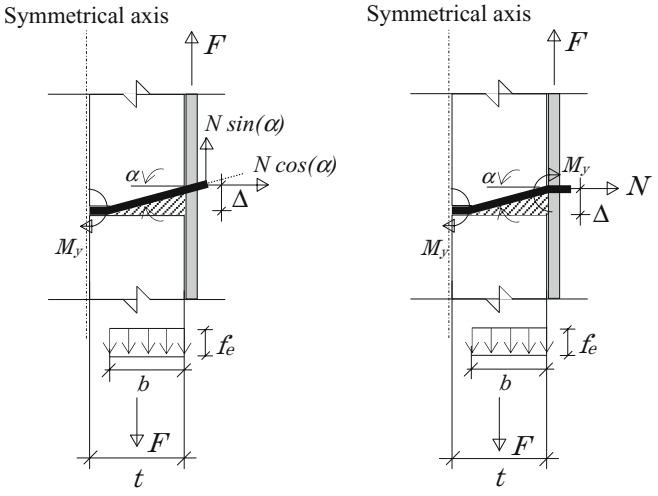

(a) Failure mode k (b) Failure mode m

Fig. 1a, b. Two possible failure modes of steel-to-timber joints with outer steel plates and slender dowel-type fastener. **a** Mode k, **b** mode m. N, Fastener's axial force; F, joint load-carrying capacity; Δ, joint slip; α, fastener bending angle; M_y, fastener's bending yield moment; f_e, dowel bearing strength; t, wood thickness

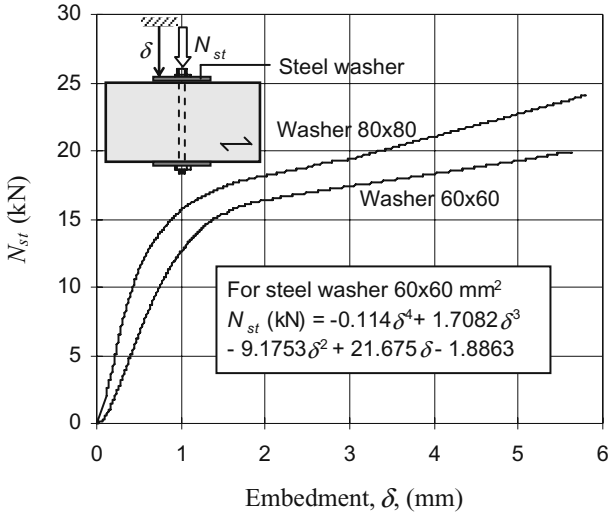

Fig. 2. Load–embedment curves of two square washers of different size.[14] δ, Steel washer embedment; N_{st}, fastener's axial force due to steel plate embedment into wood member

standards such as EC5[6] and are affected by bolt diameter, wood density, and loading direction relative to the grain. Examination of failure modes in Fig. 1 indicates that bolt end fixity will likely preclude failure mode k in double shear joints. The only exception to this would be with thin wood side members and a large bolt diameter. Based on the equilibrium condition resulting from the free body diagram of a bolt in failure mode m (see Fig. 1b), the load-carrying capacity for each shear plane is expressed as

$$F = f_e bd + \mu N \tag{1}$$

where μ is the coefficient of static friction and greatly depends on many variables,[7] and d and N are fastener diameter and the fastener axial force, respectively. In Eq. 1, b shows the thickness of the wood member that is assumed to reach the ultimate bearing strength and can be obtained as

$$2M_y + N\Delta = f_e bd\frac{b}{2}; \qquad b = \sqrt{\frac{4M_y + 2N\Delta}{f_e d}} \tag{2}$$

where Δ indicates the joint slip or displacement and M_y is the bending yield moment of the fastener.

The ultimate deformation of bolted joints cannot be determined rigidly because the deflection curve of bolts are different from each other, which results from a combination of bending stiffness, length of bolts, and bearing properties of timber. Due to this fact, it is very difficult to define the maximum resistance from the geometrical consideration. However, If the load-carrying capacity is determined by testing according to EN 26891,[8] the connection resistance is defined as the maximum load before a slip of 15 mm parallel to the load direction is reached. Bending angle of the fastener (α) at 15-mm slip can be obtained as

$$\alpha = \arctan\left(\frac{15}{b}\right) \tag{3}$$

The bending yield moment of the fastener is expressed by Eq. 4 where f_{yb} is the bending yield stress of the fastener that is set as the average between the yield and ultimate tensile stresses, and β is the plasticity index of the fastener. In Eq. 4, β equals 1.0 if the plastic hinge of the fastener is fully developed. When the bending yield moment of the fastener that corresponds to $\beta = 1.0$ is assumed to occur as the fastener bending angle equals 45°, the relationship between β and α shown by Eq. 5 can be extracted from the work of Blass et al.[9] However, for most experimental results where the failure modes occurred as shown in Fig. 1, the bending angle was significantly less than 45°.[10]

$$M_y = \frac{\beta f_{yb} d^3}{6} \tag{4}$$

$$\beta = (0.866 + 0.00295\alpha)(1 - \exp(-0.248\alpha / 0.866)) \tag{5}$$

To obtain more rational load-carrying capacity, the fastener's axial force (N) should also include the axial force reduction due to steel plate embedment into the wood member besides the fastener's pretension force. Additional shear resistance caused by steel plate embedment into the wood member, commonly known as secondary fastener's axial force,[11–13] could be predicted when the load–embedment curve of timber under a steel plates/washer is available. Typical load–embedment curves of *Picea jezoensis* (air-dry specific gravity: 0.41; moisture content: 13%) under two different square steel washers: 60-mm and 80-mm widths with 4.3 mm of thickness are shown in Fig. 2.[14] The steel plate embedment into wood member (δ) of a bolted joint with failure mode m could be approximated based on the deflection curve of the fastener and is expressed as

$$\delta = \left(\sqrt{\Delta^2 + \frac{\Delta^2}{\tan^2\alpha}} - \frac{\Delta\cos^2\alpha}{\sin\alpha}\right)\cos\alpha = \Delta\sin\alpha\cos\alpha \tag{6}$$

The fastener's axial force due to steel plate embedment into the wood member is one important source of joint strength increase described as the "rope effect."

The dependence between the fastener's bending yield moment (M_y) and the fastener bending angle (α) may be taken into account by an iterative procedure. Initially, α is set to 45°, and the plasticity index (β) and fastener's bending yield moment (M_y) can be evaluated from Eq. 5 and Eq. 4. b is computed according to Eq. 2 where the joint slip (Δ) equals 15 mm, and the fastener's axial force consists of pretension force (N_{pt}) and secondary fastener's axial force due to steel plate embedment into the wood member (N_{st}). N_{st} can be evaluated using the fourth-order polynomial expression in Fig. 2 based on the steel plate embedment given in Eq. 6. Finally, the new value of α can be calculated by solving Eq. 3. After repeating this procedure several times, the difference between the fastener bending angle of one step and that of the previous step becomes very small, less than 1°.

Figure 3 shows the fastener bending angle decreases as the fastener's axial force is increased. In the analysis, the secondary fastener's axial force caused by the steel plate embedment into the wood member (N_{st}) was evaluated based on the load–embedment curve of steel washers (60 × 60 mm) shown in Fig. 2. Significant decrease of the fastener bending angle is found when the fastener's axial force due to pretension force and that caused by steel plate embedment into the wood member were considered. When the pretension force is very large, the difference of fastener bending angle evaluated with and without the secondary fastener's axial force becomes very small. However, applying very large pretension force to the fastener is rarely found because wood beneath the steel plate would crush immediately and the amount of stress relaxation would be significant.[3,15]

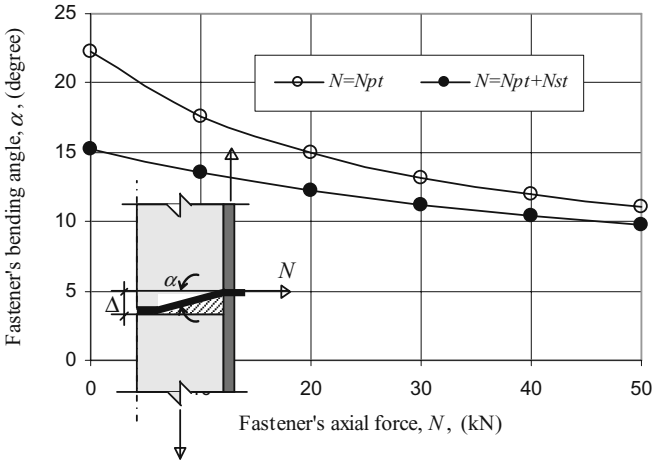

Fig. 3. Predicted fastener bending angle (α) with respect to fastener's axial force. N_{pt}, Fastener's pretension force; Δ = 15 mm

Finite element analysis

Symmetry joint configuration as shown in Fig. 4a was considered, so only half of the fastener length was modeled in the analysis. A finite fastener element of length L between nodes i and j under wood pressure $p(x)$ is illustrated in Fig. 4b. An axial spring of stiffness k_a was added to the system stiffness and its magnitude was equal to the slope of the load–embedment curve of timber under a steel washer. The finite element (FE) code DOWEL that represents the fastener as an elasto-plastic beam on a wood foundation was used in this study. The bearing behavior of the wood foundation was simulated according to Foschi's model[16,17] and it was distributed along the length of the elasto-plastic beam. Some boundary conditions were imposed on the model to simulate the failure mode m. Axial displacement and bending rotation of the node at the symmetrical axis were restrained, and bending rotation at the node next to the steel plate member, which may occur due to lead-hole clearance, was restrained. Stepwise displacement loading control was implemented in this finite element analysis through imposing small increments of lateral displacement at the node next to the steel plate member. The analysis was stopped when the joint load-carrying capacity had decreased to 80% of the maximum load.

Materials and methods

Double-shear tests of single-bolt timber joints with steel side plates were conducted on spruce–pine–fir glued laminated timber. Three different pretension forces: 0, 4.0, and 9.2 kN were applied to the bolt before the joints were laterally loaded. By considering the contact area between the steel plate and wood member, the prestress level on the

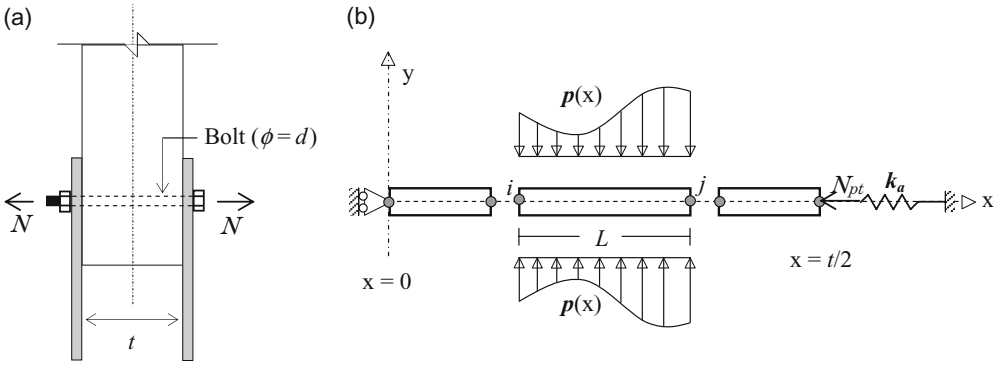

Fig. 4. **a** Bolted joint under consideration and **b** its finite element model. d, Bolt diameter; $p(x)$, wood pressure; k_a, spring constant; L, length of finite element between nodes i and j

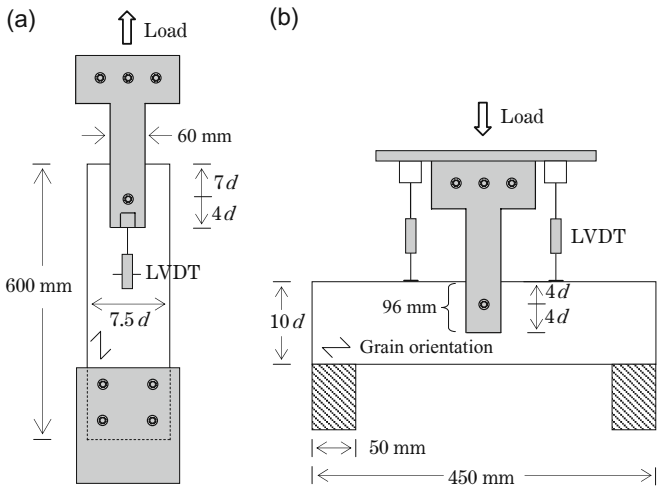

Fig. 5a, b. Test setup of double shear timber joint: **a** loading parallel to the grain; and **b** loading perpendicular to the grain. $d = 12$ mm; steel plate thickness = 4 mm; wood member thickness = 100 mm; *LVDT*, displacement transducer

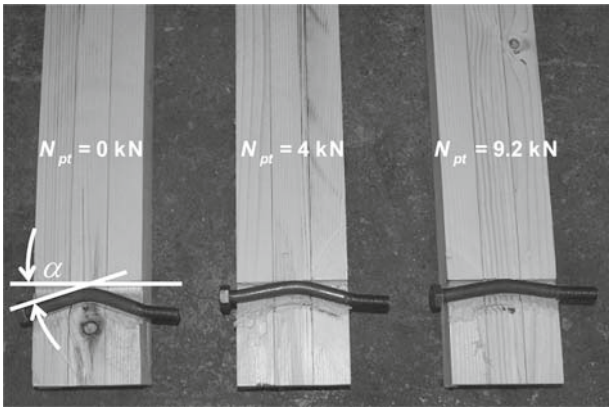

Fig. 6. Measurement of fastener bending angle (α)

wood member due to bolt pretension of 4.0 and 9.2 kN approximately equals 0.7 and 1.6 MPa, respectively. A prestress level of 0.7 MPa is the minimum level recommended by AASTHO[18] to prevent interlayer slip among the laminations, while a prestress level of 1.6 MPa is about 90% of the allowable long-term edge-bearing strength of spruce species.[19] Six replicates were prepared for each combination and all wood specimens were derived by a matched sample technique; one specimen of each three different pretension forces was obtained from the adjacent location in a single glued laminated timber. A lead hole that was 1 mm larger than the bolt diameter was drilled on both wood and steel members to accommodate the actual practice of joint assembly.[20] All specimens were tested to failure at a constant displacement rate of 1.2 mm/min by using the test setup shown in Fig. 5 where the joint slip was obtained by averaging two continuous slip measurements. In all specimens, end and edge distances satisfied the minimum requirements given in NDS.[21]

After the test, a small wood specimen was cut from the vicinity of the connection to determine moisture content and specific gravity of the specimen. The average moisture content was found to be 10%, while the air-dry and oven-dry specific gravity was 0.41 and 0.37, respectively. Monotonic tension tests on three replicates of 12-mm-diameter bolts showed an average ultimate tensile strength and 0.2% offset yield strength of 440 and 386 MPa, respectively. The tensile stress in the bolt due to pretension force of 4.0 kN or 9.2 kN was about 35 MPa or 81 MPa, and these stresses were far less than the proportional tensile stress (273 MPa). A friction test was carried out to evaluate the coefficient of static friction between the steel plate and the wood member. In the friction test, the horizontal force required to slide a wooden block with a surface measuring 200 × 200 mm that was subjected to a distributed vertical load was measured. The coefficient of static friction was the ratio of the horizontal force with respect to the vertical load. This coefficient varied from 0.28 to 0.34 with an average value of 0.30.

Results and discussion

Direct measurement of fastener bending angle was carried out after completing the test as shown in Fig. 6 and all bolted joints were found to have failed according to failure mode m. Significant bending deformation of bolt with more than one possible plastic hinge and partial bearing damage of the wood member beneath the bolt were visually observed. Following this inelastic deformation, wood splitting due to high shear forces inside the joint ended the test. Among all the tested joints, none failed due to premature splitting or failure without remarkable inelastic deformation. The experimental load–slip curve shown in Fig. 7 shows that the joints under loading parallel to the grain failed with a slip averaging 15 mm, while for loading perpendicular to the grain, only a few joints reached 15-mm displacement. Based on the experimental fastener bending angles summarized in Table 1, it can be observed that the fastener bending angle of the joints decreased as the magnitude of the pretension force was increased. This decrease of fastener bending angle is essentially due to significant frictional resistance between wood and steel members found in the pretensioned joints as one of the joint strength components besides bending of the fasteners and bearing of the wood around the bolt.

The predicted fastener bending angle given in Fig. 3 was still higher than that of the experiment because the fastener's elastic bending deformation recovered after the test, and some joints especially that were loaded perpendicular to the grain reached their ultimate load before a slip of 15 mm. Determination of joint load-carrying capacity based on a slip of 15 mm therefore requires special conditions as follows: (1) bolted joints with loading perpendicular to the grain should be tested with an edge distance of more than 4*d*; and (2) a high ratio of wood member thickness to fastener diameter is required to ensure that the failure modes shown in Fig. 1 can be adopted. As the magnitude of fastener pretension increases, the area of wood beneath the

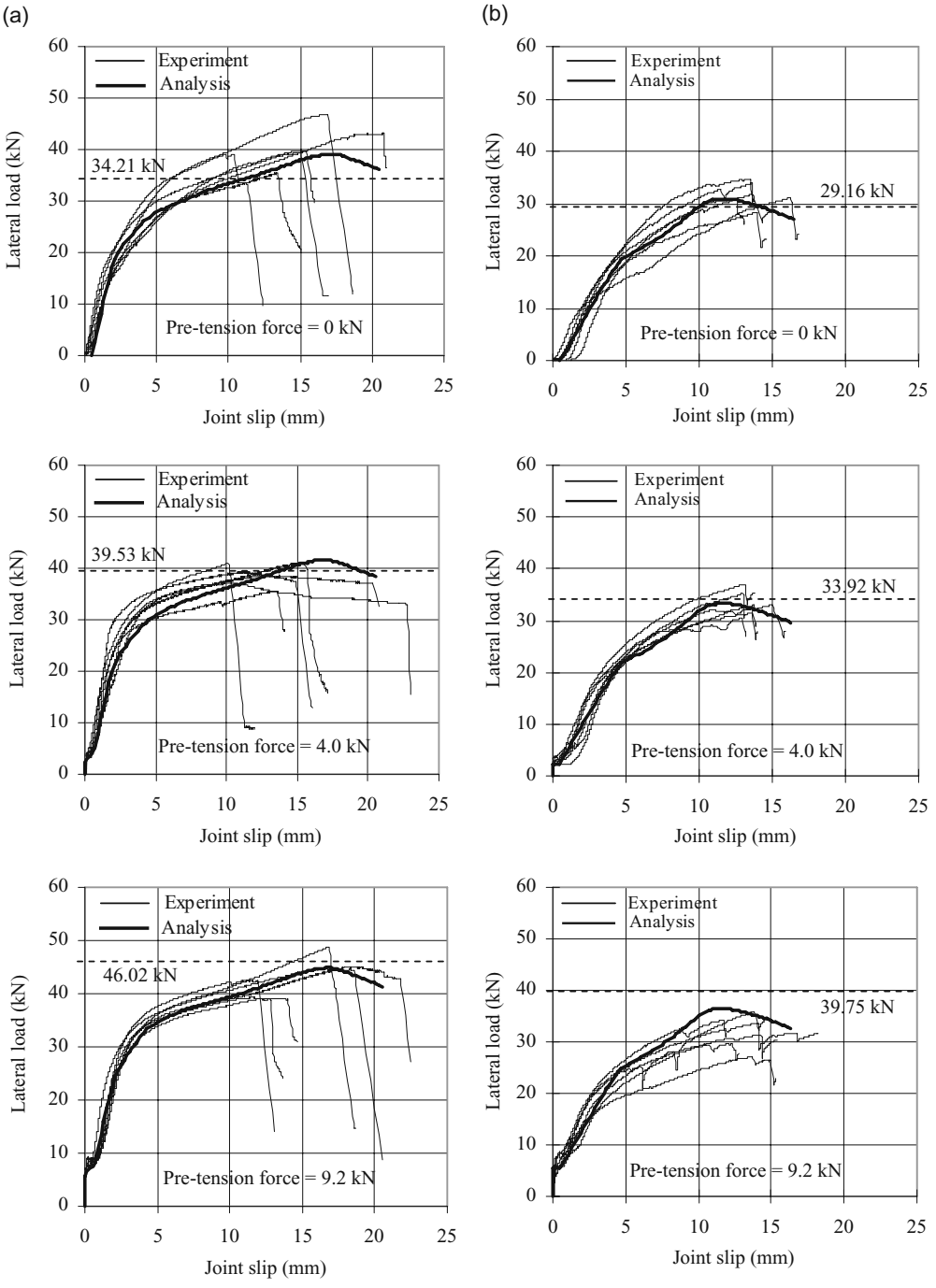

Fig. 7a, b. Analyzed and experimental load–slip curves with different fastener pretension forces: **a** loading parallel to the grain; and **b** loading perpendicular to the grain. *Dotted horizontal lines* show load-carrying capacity on the basis of proposed extended yield model

Table 1. Experimental fastener bending angle and load-carrying capacity

Loading to grain	N_{pt} (kN)	Bending angle (degrees)	Yield load[a] (kN)	Ultimate load[b] (kN)
Parallel	0.0	10.2 (8.1–14.0)	29.38 (26.88–32.50)	39.96 (35.43–46.00)
	4.0	8.6 (6.7–9.9)	32.22 (28.44–34.06)	38.62 (35.51–40.94)
	9.2	6.8 (5.7–8.1)	34.58 (33.75–35.94)	42.54 (39.07–47.10)
Perpendicular	0.0	5.4 (4.3–6.7)	21.33 (18.19–26.67)	31.65 (28.25–34.58)
	4.0	4.9 (3.8–5.7)	24.40 (22.26–27.42)	33.11 (30.50–37.05)
	9.2	3.8 (1.5–4.7)	22.55 (17.81–25.00)	31.89 (27.06–35.71)

Values in parentheses are minimum and maximum values
N_{pt}, Fastener's pretension force
[a] Load at the intersection of the tangents to the linear and nonlinear portion of the load–slip curve
[b] Maximum load before a joint slip of 15 mm

fastener that is assumed to reach ultimate bearing strength becomes larger.

Experimental load–slip curves presented in Fig. 7 clearly show that the joint resistances during initial loading or small joint slip increase as the pretension force is increased. This joint resistance during initial loading is entirely due to static friction between the steel plates and the wood member. Afterward, sudden decrease of stiffness was found in the load–slip curve of the pretensioned joints as an indication of slip between the steel plates and the wood member. Following this slip occurrence, tangents of the load–slip curves of both pretensioned and nonpretensioned joints were comparable and reflected composite action of the elasto-plastic beam on the wood foundation model. The average lateral load at this slip occurrence was 3.36 kN and 6.92 kN for the bolted joint with 4.0 kN and 9.2 kN of pretension force, respectively. These frictional resistances were about 25% and 40% higher than the calculation using 0.30 of the static friction coefficient. This increase is probably due to an increase in the static friction coefficient between wood and steel members as the timber members were tested under double-shear test configuration. In the joint test, it was not possible for the stress perpendicular to the grain to be equally distributed on the contact surfaces, while in the friction test the stress was almost equally distributed.

Figure 7 shows that additional shear resistance due to steel plate embedment into the wood member, which is most obviously indicated by the tangent of the nonlinear portion of the curve, was found to be small in the case of pretensioned joints. Decrease of shear resistance contributed by steel plate embedment into the wood member is closely related to the reduction of the fastener bending angle as the fastener was pretensioned. This fact can also be observed from the ratio of the yield load to the ultimate load-carrying capacity presented in Table 1. For the nonpretensioned joints, this ratio was about 0.73 and 0.67, respectively, for loading parallel and perpendicular to the grain. In the case of pretensioned joints, this ratio was 0.83 and 0.74 for loading parallel and perpendicular to the grain, respectively. The finite element analysis carried out in this study did not consider the additional load-carrying capacity caused by frictional resistance that corresponds to fastener's pretension force, so the obtained load–slip curves were modified accordingly. The curve was derived by adding the frictional resistance to the lateral load data of any joint slip point given by the analysis.

The joint load-carrying capacity of Eq. 1 was evaluated based on a joint slip of 15 mm and a static friction coefficient of 0.3. This joint load-carrying capacity is presented in Fig. 7 together with the experimental load–slip curves. It can be observed from Table 2 that the ratios between the computed and experimental average results increased with force pretension. Some of the observed load-carrying capacities of the joints, particularly for loading perpendicular to the grain, were not as high as those expected by the numerical analyses considering the given pretension forces. This suggests that the effect of pretensioning is probably overestimated. Moreover, it should be taken account that the axial pretension force is not constant during the test, but

Table 2. Ultimate loads computed on the basis of proposed extended yield model

Loading to grain	N_{pt} (kN)	Computed ultimate load (kN)	Ratio with average
Parallel	0.0	34.21	0.856
	4.0	39.53	1.024
	9.2	46.02	1.082
Perpendicular	0.0	29.16	0.921
	4.0	33.92	1.024
	9.2	39.75	1.246

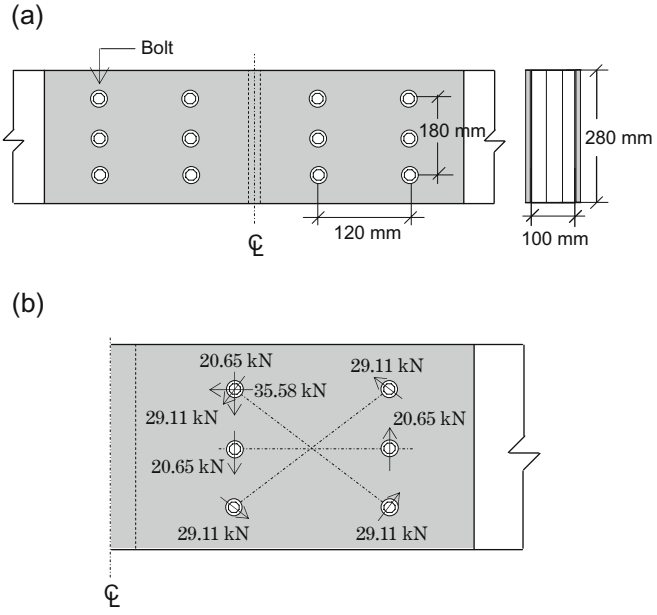

Fig. 8a, b. Moment-resisting joint tested by literature method:[4] **a** geometry of joint; and **b** lateral force of each fastener of the pretensioned joint due to 0.054 radians of joint rotation

decreases as a consequence of dowel lateral deformation. Besides the load-carrying capacity obtained from the extended yield model and the experimental load–slip curve, Fig. 7 shows the load–slip curve obtained from the FE analysis. Good agreement was found between the experimental and the analyzed load–slip curves, although the FE model ignored the lateral compressive stress on the wood member due to axial pretensioning. It is possible that the lateral compressive stress caused by pretension force was surpassed by the compressive stress of steel plate embedment into the wood member resulting from dowel deformation. Both the experimental and analyzed load–slip curves shown in Fig. 7 well indicate that the joint slip that corresponds to the ultimate load-carrying capacity seems to be negatively influenced by the pretension application.

Results of this experiment were utilized to predict the maximum resistance of moment-resisting timber joints tested in our previous work.[4] The mechanical properties of the wood member, steel fasteners, and steel plates used in our previous work were the same as those of this study. In our previous work, moment-resisting joints as shown in Fig. 8a with two different prestress levels of 0 kPa and

1.6 MPa were tested. Maximum moment resistance and its corresponding joint rotation of the nonpretensioned joints were found to be 13.42 kNm and 0.073 radians, respectively. In the case of pretensioned joints, the maximum moment resistance and its corresponding joint rotation were, respectively, 14.87 kN and 0.054 radians. Figure 8b shows the lateral force of each fastener in the pretensioned joints that corresponds to 0.054 radians of joint rotation. These lateral forces were obtained from Fig. 7 (curves with pretension force of 9.2 kN) where the fastener slip was attained by multiplying the joint rotation by the distance of the fastener to the geometric centroid of rotation. The Hankison formula was used to evaluate the lateral force when its angle to the grain was neither parallel nor perpendicular. The moment resistance that was determined by summing the product of the force acting on each bolt and the distance of the bolt to the centroid of the bolt group was found to be 13.81 kNm and 15.08 kNm, respectively, for the nonpretensioned and pretensioned joints. These predicted moment resistances were about the same as the experimental results of our previous work.

Conclusions

The introduction of pretension force in the bolt greatly increases the joint resistance at the initial loading stage due to frictional resistance between the joint members. Failure modes of the joints with and without axial pretension force in general were similar, but the pretensioned joints failed with a smaller fastener bending angle than the nonpretensioned joints. With large joint slip, therefore, the pretensioned joints had small tangential slopes, indicating less additional shear resistance due to steel plate embedment into the wood member. By taking the fastener's axial forces into consideration, the extended yield model developed in this study slightly overestimated the joint load-carrying capacity, especially for loading perpendicular to the grain. This is because the applied pretension force is not constant during the test, but decreases as a consequence of dowel lateral deformation. After modifying the analytical load–slip curve to take into account the additional shear strength caused by static frictional resistance, good agreement was found between the experimental and analyzed load–slip curves.

Acknowledgments A.A. thanks the Japan International Cooperation Agency (JICA) through AUN/SEED-Net program for provision of an educational scholarship.

References

1. Ritter MA, Wacker JP (1995) Field performance of stress-laminated timber bridge on low-volume roads. Proceeding of International Conference on Low-Volume Roads, 25–29 June, Minneapolis, vol 2, pp 347–356
2. Wipf TJ, Ritter MA, Wood DL (1999) Dynamic evaluation and testing of timber highway bridges. Proceedings of Pacific Timber Engineering Conference, 14–18 March, Rotorua, vol 3, pp 333–340
3. Quenneville JHP, Dalen KV (1991) The enhanced performance of split-ring connections through prestressing. Can J Civ Eng 18: 830–838
4. Awaludin A, Hirai T, Toshiro T, Sasaki Y, Oikawa A (2007) Effects of pretension in bolts on hysteretic responses of moment-carrying timber joints. J Wood Sci 54:114–120
5. Schreyer AC (2002) Monotonic and cyclic behavior of slender dowel-type fasteners in wood-steel-wood connections. M.A.Sc. Thesis, Department of Wood Science, University of British Columbia
6. British Standards Institution (2004) BS EN 1995-1-1:2004, Eurocode 5 – design of timber structures – part 1-1: general-common rules and rules for buildings. London
7. Chang WS, Komatsu K, Hsu MF, Chen WJ (2007) On mechanical behavior of timber shear wall in Taiwan. J Wood Sci 53:17–23
8. European Committee for Standardization (1991) EN 26891: timber structure – joints made with mechanical fasteners: general principle for the determination of strength and deformation characteristics. European Committee for Standardization, Brussels
9. Blass HJ, Bienhaus A, Kramer V (2000) Effective bending capacity of dowel-type fasteners. Proceedings of the 33rd CIB-W18, Delft
10. Jorissen A, Blass HJ (1998) The fastener yield strength in bending. Proceedings of the 31st CIB-W18, Savonlinna
11. Hirai T (1991) Analysis of the lateral resistance of bolt joints and drift-pin joints in timber II: numerical analysis applying the theory of a beam on an elastic foundation (in Japanese). Mokuzai Gakkaishi 37:1017–1025
12. Kamachi K, Ando N, Inayama M (2006) New method to estimate the load–slip characteristics of the double-shear bolted timber-to-timber joints. Proceedings of World Conference on Timber Engineering, August 6–10, Oregon
13. Nishiyama N, Ando N (2003) Analysis of load–slip characteristics of nailed wood joints: application of a two-dimensional geometric nonlinear analysis. J Wood Sci 49:505–512
14. Hirai T, Tsujino T, Sasaki Y (2006) Steel washers on timber. Proceedings of World Conference on Timber Engineering, August 6–10, Oregon
15. Manrique RE (1969) Stress relaxation of wood at several levels of strain. J Wood Sci Technol 3:49–73
16. Foschi RO (1974) Load–slip characteristics of nails. J Wood Sci 7:69–74
17. Prion H, Foschi R (1994) Cyclic behaviour of dowel type connections. Proceedings of Pacific Timber Engineering Conference, 11–15 July, Gold Coast
18. American Association of State Highway Officials (1991) Guide specifications for the design of stress-laminated wood decks. American Association of State Highway Officials, Washington DC
19. Architecture Institute of Japan (2006) Standard for structural design of timber structures. Architecture Institute of Japan, Tokyo, pp 13–14, p 400
20. American Society for Testing and Materials (1994) Standard test methods for bolted connection in wood and wood-base products. ASTM section D07.05.02, Draft 8, American Society for Testing and Materials, Philadelphia
21. American Society of Civil Engineers (1997) National design and specification for timber construction of US. American Society of Civil Engineers, New York